

Electrical transport and anisotropic superconducting properties in single crystalline and dense polycrystalline MgB₂

A. K. Pradhan,* Z. X. Shi, M. Tokunaga, and T. Tamegai†

Department of Applied Physics, The University of Tokyo, Hongo, Bunkyo-ku, Tokyo 113-8656, Japan

Y. Takano and K. Togano

National Institute for Materials Science, 1-2-1 Sengen, Tsukuba 305-0047, Japan

and CREST, Japan Science and Technology Corporation, 2-1-6 Sengen, Tsukuba 305-0047, Japan

H. Kito and H. Ihara

National Institute of Advanced Industrial Science and Technology, 1-1-1 Umezono, Tsukuba 305-8568, Japan

(Received 8 June 2001; published 13 November 2001)

The transport properties of dense polycrystalline and single-crystalline MgB₂ platelets have been measured to determine the effects of grain size on the upper critical field H_{c2} and the anisotropy parameter. The H_{c2} in polycrystalline MgB₂ is enhanced and the magnetic-field-induced broadening is significantly reduced with increasing grain size, probably due to reduced contamination at the grain boundaries. Single-crystalline MgB₂ exhibits remarkable anisotropy in $H_{c2}(T)$ and irreversibility field $H^*(T)$ with anisotropy $\gamma = H_{c2}^{ab}/H_{c2}^c \sim 3 \pm 0.2$. The large broadening of the superconducting transition for the $\mathbf{H}||c$ direction indicates a significant suppression of $H^*(T)$ below H_{c2}^c , giving $H^{*c}(T) \sim 0.71H_{c2}^c(T)$.

DOI: 10.1103/PhysRevB.64.212509

PACS number(s): 74.25.Fy, 74.60.Ec, 74.60.Ge, 74.62.Bf

The recent discovery¹ of superconductivity in MgB₂ with a transition temperature of about 39 K has generated extensive scientific interest for both basic and applied research. From studies of several fundamental properties, it is now apparent that MgB₂ is a type-II superconductor with $\lambda \sim 140$ nm and upper critical field $H_{c2}(0) \sim 16$ –18 T, while the irreversibility field H^* is about $0.5 H_{c2}$.^{2–8} An issue of primary importance is to what degree this superconductor is anisotropic. Since MgB₂ consists of alternating B and Mg sheets, electronic anisotropy has been anticipated.⁹ For hot-pressed samples,¹⁰ partially oriented crystallites,¹¹ and c -axis-oriented thin films,¹² the upper critical field anisotropy ratio $\gamma = H_{c2}^{ab}/H_{c2}^c$ is reported as 1.1, 1.7, and about 2, respectively. Very recently, an anisotropy ratio ranging from 1.7 to 2.7 was determined in single crystals.^{13–15} However, the actual value of γ and its upper limit remain unresolved, the reason being the different qualities of single crystals and significant normal-state magnetoresistance. The anisotropic nature of MgB₂ will strongly affect the irreversible properties, especially the irreversibility field $H^*(T)$ at which the bulk supercurrent density disappears. Hence studies of the anisotropic properties of MgB₂ in its different forms are currently of potential interest both for physics and application points of view.

The other interesting features concerning the electronic transport in the mixed state and the broadening of the superconducting transition in applied magnetic fields have drawn attention to flux pinning. On the other hand, the anomalous behavior of the Hall coefficient^{16–18} raises questions related to the nature of carriers. Since MgB₂ looks promising for applications, the influence of a moderately high anisotropy value on the electrical transport and its implications for flux pinning in bulk, thin films, and single crystals are of tremendous importance. Although weak-link phenomena seem to be

much less operative in MgB₂ compared to high- T_c cuprates,⁴ grain size effects on various physical properties remain a nontrivial problem.

In this communication, we report on the electronic transport properties of dense polycrystalline bulk and single-crystalline MgB₂ over a wide temperature range from 300 to 5 K. The H_{c2} is enhanced and the magnetic-field-induced broadening is significantly reduced in MgB₂ with increasing grain size in the bulk due to reduced contamination and impurities. Single-crystalline MgB₂ exhibits remarkable anisotropy in $H_{c2}(T)$ and $H^*(T)$ with $\gamma = H_{c2}^{ab}/H_{c2}^c \sim 3 \pm 0.2$. The large broadening of the superconducting transition for the $\mathbf{H}||c$ direction indicates a significant suppression of $H^*(T)$ below H_{c2}^c for the same orientation.

The highly dense (density ~ 2.63 g/cm³) MgB₂ bulk samples (MgB₂ No. 1 and MgB₂ No. 2) were synthesized under high pressure (3.5 GPa) at high temperature (1000 °C) in BN crucible as described earlier.⁵ Higher-purity starting materials were used for the synthesis of MgB₂ samples (MgB₂ No. 2) and the details will be published elsewhere.¹⁹ X-ray diffraction reveals that the sample is single phase. The high-resolution polarizing microscope reveals grains of size 1–5 μm in MgB₂ No. 1, whereas 50–200 μm long grains were seen in MgB₂ No. 2. Magnetization and micro-Hall-probe measurements show a superconducting transition T_c between 37.5 and 38.2 with $\Delta T_c < 1$ K. Shiny golden-yellow-colored single-crystalline MgB₂ platelet samples of dimensions $250 \times 100 \times 40$ μm^3 were extracted from MgB₂ No. 2 for transport measurements. The resistively measured T_c was found to be at ~ 38.2 K with $\Delta T_c \sim 0.3$ K. Field-dependent resistivity was measured using a standard four-probe ac technique ($f = 16$ Hz). Current-voltage (I - V) measurements were performed by the dc method with the current reversal technique.

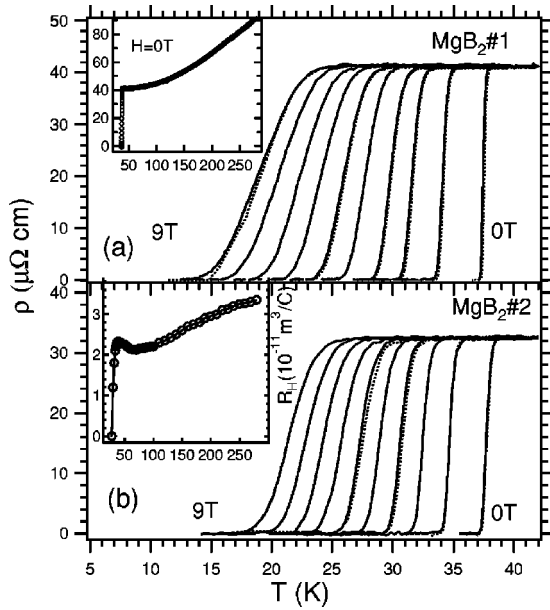


FIG. 1. Temperature-dependent electrical resistivity of (a) MgB₂ No. 1 and (b) MgB₂ No. 2 in both perpendicular (solid lines) and parallel fields (dashed lines) $H=0, 1, 2, 3, 4, 5, 6, 7, 8,$ and 9 T (right to left), respectively. The inset in (a) shows the temperature dependence of the normal-state resistivity of MgB₂ No. 1 for $H=0$ T. The inset in (b) shows the temperature dependence of the Hall coefficient of MgB₂ No. 2.

First, we discuss the behavior of field-induced resistive transitions in MgB₂ No. 1 and No. 2. In Fig. 1 we present the resistive superconducting transition in MgB₂ No. 1 and MgB₂ No. 2 under both perpendicular (solid lines) and parallel (dashed lines) magnetic fields, both perpendicular to the current flow, up to 9 T. The temperature-dependent electrical resistivity ρ of MgB₂ No. 1, shown in the inset of Fig. 1(a), roughly obeys the power law $\rho = \rho_0 + \rho_1 T^\alpha$ with $\alpha \sim 1.9$, in the normal state. Similar behavior with $\alpha \sim 2.1$ was found in MgB₂ No. 2. The resistivity $\rho(40 \text{ K}) \sim 41.7 \mu\Omega \text{ cm}$ in MgB₂ No. 1 is reduced to $\sim 32.1 \mu\Omega \text{ cm}$ for MgB₂ No. 2. The magnetotransport results show two significant differences between two types of samples. In MgB₂ No. 1, there is a large broadening in resistivity under magnetic field with a pronounced tail feature, indicating a considerable flux-flow phenomenon observed in sintered MgB₂ bulk.² This behavior is strongly reduced in MgB₂ No. 2, as a consequence, both H_{c2} and H^* are enhanced. Note that the magnetic critical current density in MgB₂ No. 2 is enhanced by an order of magnitude ($\sim 1 \times 10^4 \text{ A/cm}^2$) at 5 K in a field of 5 T compared to that of MgB₂ No. 1. Although weak links are the primary suspects of such a large resistive broadening, contamination due to foreign atoms might play a major role. No significant anisotropy was observed in both samples as shown in Fig. 1 for two field orientations, which is consistent with a random orientation of each grain in the polycrystalline pellets.

In the inset of Fig. 1(b), we show the temperature dependence of the Hall coefficient R_H of MgB₂ No. 2, calculated under magnetic field reversal ($H = \pm 5$ T) at a given temperature. R_H is positive over the whole temperature range

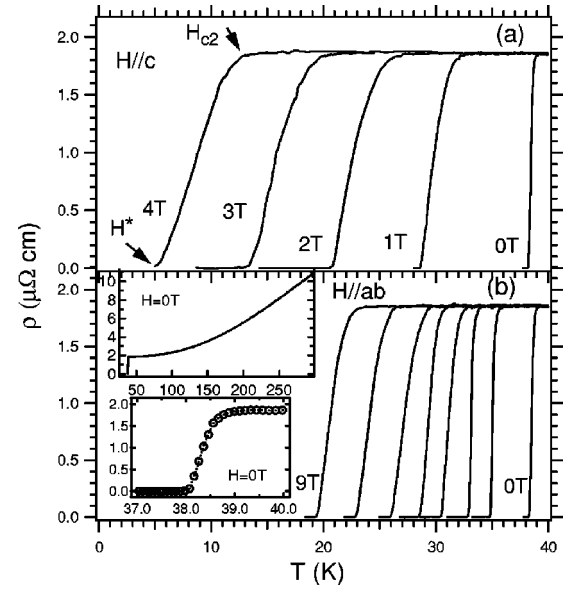


FIG. 2. Temperature dependence of the in-plane resistivity at various magnetic fields (a) up to 4 T for $\mathbf{H}||c$ axis, (b) for $\mathbf{H}||ab$ axis at $H=0, 1, 2, 3, 4, 5, 7, 9$ T in a MgB₂ single-crystalline sample. The upper inset in (b) shows the temperature dependence of the normal state resistivity for $H=0$ T. The lower inset in (b) shows the temperature dependence of the resistivity near the transition.

and is weakly temperature dependent. R_H shows a peak around T_c before going to zero without any sign change anomaly. This is consistent with the recent report on thin film¹⁷ rather than that for a polycrystalline sample.¹⁶ The estimated hole carrier density $\sim 1.84 \times 10^{23} \text{ holes/cm}^3$ at 300 K is rather high and needs its explanation using a two-band model; however, it is consistent with the low resistivity observed in MgB₂. We estimate the mean free path at the lowest temperature $l = 90 \text{ nm}$ from $l = 3[\rho N(0) v_F e^2]$, where ρ is the residual resistivity, $N(0)$ is the density of states at the Fermi level, v_F is the Fermi velocity, and e is the elementary charge. Here we used $N(0) = 0.7 \text{ states/(eV cell)}$ from specific heat measurement,²⁰ and $v_F = 4.8 \times 10^7 \text{ cm/sec}$ from band structure calculations.²¹ The coherence length without impurity is given by $\xi_0 \sim 0.18 \hbar v_F / k_B T_c$ and is estimated as 17 nm. With these estimations, we can safely claim that our MgB₂ single crystal is in the clean limit $l/\xi_0 > 1$.

Figure 2 shows the main results of this paper. The temperature-dependent resistivity curves are shown for fixed field values applied in both the (a) $\mathbf{H}||c$ and (b) $\mathbf{H}||ab$ planes of the MgB₂ single-crystalline sample. The estimated resistivity ratio $\rho(300 \text{ K})/\rho(40 \text{ K})$ is ~ 5.5 with $\rho(40 \text{ K}) \sim 1.8 \mu\Omega \text{ cm}$. This value is much smaller than our polycrystalline samples, but similar to the results on single crystals.¹³⁻¹⁵ The temperature dependence of the resistivity in zero field shown as an inset in Fig. 2(b) roughly obeys a $\rho = \rho_0 + \rho_1 T^\alpha$ power law with $\alpha \sim 3$ in the normal state and is consistent with a previous report.² A sharp T_c at ~ 38.2 K with $\Delta T_c < 0.3$ K indicates the high quality and homogeneity of the crystal. Although T_c of the present crystal is slightly lower than that of bulk¹ and wires,⁶ it is very similar

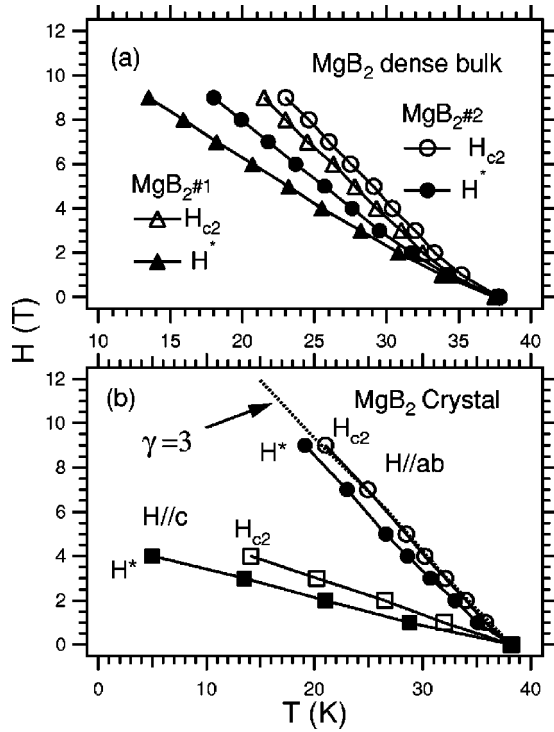


FIG. 3. Temperature dependence of the upper critical fields H_{c2} and irreversibility fields H^* of (a) MgB₂ No. 1 and MgB₂ No. 2, and (b) single-crystalline MgB₂.

to single-crystal results.^{13–15} The origin of a lower T_c in single crystals may be related to unavoidable contamination by impurities from the BN (Refs. 5 and 15) containers, when using cubic anvil and Mo (Ref. 13) or Nb (Ref. 14) in other cases. The resistive transition under magnetic field for $\mathbf{H}||c$ is significantly suppressed compared to that for $\mathbf{H}||ab$. In addition, the significant broadening of the transition for $\mathbf{H}||c$ causes a large suppression of H^* . Interestingly, the transition remains very sharp for the $\mathbf{H}||ab$ plane, indicating a moderately large upper critical field anisotropy in the system. Figure 3 shows in detail the resistively determined $H_{c2}(T)$ and $H^*(T)$ lines for dense pellets and single-crystalline MgB₂ samples. $H^*(T)$ defined with a criterion of $\rho = 0.01 \mu\Omega \text{ cm}$ is shown in Fig. 2(a) as arrows. Thus determined $H^*(T)$ roughly coincides with that determined from magnetic measurements with a critical current criterion of $J_c = 100 \text{ A/cm}^2$.

It is clear that both $H_{c2}(T)$ and $H^*(T)$ in MgB₂ No. 2 are higher than that of MgB₂ No. 1. The suppression of $H^*(T)$ is remarkably smaller in MgB₂ No. 2, indicating reduced flux flow and weaker vortex fluctuations. In MgB₂ No. 2, H^* occurs at $H^*(T) \sim 0.72H_{c2}(T)$ which is larger than that of 0.66 estimated for MgB₂ No. 1. The higher H_{c2} values obtained in MgB₂ No. 2 can have several reasons. Consider a sample of randomly oriented grains of a uniaxial superconductor with anisotropy $\gamma = H_{c2}^{ab}/H_{c2}^c$ placed in a field along z . The distribution of grains over their c direction is given by $dN = N \sin \theta d\theta/2$ with θ being the angle between the c axis and the applied field H . It is certain that the upper critical field of the grains depends on θ according to²² $H_{c2}(\theta)$

$= H_{c2}^{ab}/\epsilon(\theta)^{1/2}$ with $\epsilon(\theta) = 1 + (\gamma^2 - 1)\cos^2\theta$. In the absence of any anisotropy in H_{c2} in both bulk samples, the observed H_{c2} is rather due to the average effects of all grains than any preferential grain orientations. This shows a lack of texturing in both bulk samples. One of the major dominating effects on both H_{c2} and H^* is due to impurities. The presence of a small amount of MgO and MgB₄ at grain boundaries in MgB₂ No. 1 (Ref. 8) may be one of the reasons for reduced H_{c2} and H^* and enhanced dissipation. In contrast, MgB₂ No. 2 has large grain size and is free from such disorders. Impurities enhance carrier scattering and reduce the mean free path l . Since $H_{c2} \propto \Phi_0/\xi^2$ and ξ is related to l as $1/\xi = 1/l + 1/\xi_0$, where Φ_0 is the flux quantum and ξ_0 is the coherence length without impurities, one can argue that a reduction of l by impurities should enhance H_{c2} , which is contrary to what we observed. Hence we speculate that impurities in MgB₂ No. 1 are mainly localized near the grain boundaries and affect intergranular transport. They may also be a limiting factor for grain growth. Alternatively, atomic disorder inside the grain may be another reason for the enhancement of both H^* and the critical current density as recently found in MgB₂ upon proton irradiation.²³

In the MgB₂ single-crystalline sample [shown in Fig. 3(b)], it is immediately clear that there is a remarkable anisotropy in the upper critical fields with anisotropy ratio γ

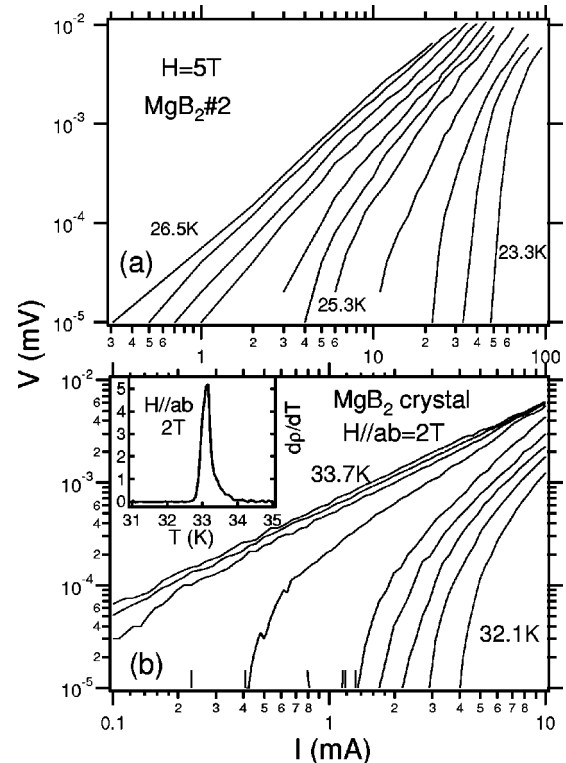


FIG. 4. Current-voltage (I - V) curves of (a) MgB₂ No. 2 for $H=5 \text{ T}$ in the temperature range 26.5–25.3 K (0.2 K step) and 25.3–23.3 K (0.5 K step) and (b) MgB₂ crystal for $H=2 \text{ T}$ applied parallel to the ab plane within the temperature range between 33.7 K and 32.1 K (0.2 K step). The inset in (b) shows the temperature dependence of $d\rho/dT$ for $\mathbf{H}||ab=2 \text{ T}$, showing a sharp transition.

$=H_{c2}^{ab}/H_{c2}^c \sim 3 \pm 0.2$, which is larger than the reported values,¹¹⁻¹⁵ but smaller than the estimation by CESR,²² $\gamma = 6-9$. A significant suppression of the irreversibility field H^* occurs for $\mathbf{H}||c$, giving $H^{*c}(T) \sim 0.71H_{c2}^c(T)$, which is larger than that of the recent report¹⁵ of $H^{*c}(T) \sim 0.5H_{c2}^c(T)$. This is mainly due to the single resistive transition observed in the present crystal for $\mathbf{H}||c$. By contrast, for $\mathbf{H}||ab$ we found $H^{*ab}(T) \sim 0.91H_{c2}^{ab}(T)$. The $H^{*c}(T)$ is also suppressed in comparison to the H_{irr} determined magnetically in a sintered sample.² We evaluated $dH_{c2}^c(T)/dT \sim -0.17$ T/K and $dH_{c2}^{ab}(T)/dT \sim -0.55$ T/K in the higher-field region in order to avoid the region of small positive curvature at low fields and to exclude any contribution from the minority phase. In addition, we mention that a small positive curvature in H_{c2} near T_c may also support that MgB₂ is a clean-limit superconductor like intermetallic borocarbides.²⁴ Assuming the extrapolation formula for an isotropic *s*-wave superconductor,⁹ $H_{c2}(0) = 0.73T_c[-dH_{c2}(T)/dT]$, we estimated $H_{c2}^c(0) \sim 4.8$ T and $H_{c2}^{ab}(0) \sim 15$ T, giving $\gamma \sim 3.2$. The simple extrapolation of H_{c2}^c and H_{c2}^{ab} lines to the zero-temperature axis yields $H_{c2}^c(0) \sim 6.5$ T and $H_{c2}^{ab}(0) \sim 20.5$ T. Using the anisotropic Ginzburg-Landau (GL) equations $H_{c2}^c(0) = \Phi_0/(2\pi\xi_{ab}^2)$ and $H_{c2}^{ab}(0) = \Phi_0/(2\pi\xi_{ab}\xi_c)$, the GL coherence lengths $\xi_c(0)$ and $\xi_{ab}(0)$ are estimated to be ~ 2.7 nm for $\mathbf{H}||c$ and ~ 8.2 nm for $\mathbf{H}||ab$. Hence, we can conclude that MgB₂ shows a moderate anisotropy that is between intermetallic borocarbides (~ 1.13) and YBa₂Cu₃O₇ (~ 6).

Finally, in Fig. 4 we present the isothermal *I-V* curves for (a) MgB₂ No. 2 at $H=5$ T and (b) single-crystalline MgB₂ at $H=2$ T applied parallel to the *ab* plane. MgB₂ No. 2 shows *I-V* curves similar to the recent report on MgB₂ films²⁵ and YBa₂Cu₃O₇, and can be consistently explained

using vortex-glass theory.²⁶ However, a scaling analysis of the vortex state is beyond the scope of the present paper. In Fig. 4(b) we show a remarkably different behavior of *I-V* curves in single-crystalline MgB₂ for $\mathbf{H}||ab$. The sudden change of the curvature may indicate a first-order-like vortex-lattice melting transition for this field orientation. The temperature dependence of $d\rho/dT$ for $\mathbf{H}||ab$ at 2 T shown in the inset of Fig. 4(b) exhibits a sharp peak, suggesting the phenomenon of melting. The transition becomes broader for higher fields possibly due to the dominant effect of disorder. The transition was found to be very weakly current dependent. It is worth mentioning that a similar sudden change of slope is observed in the same crystal in low fields, $H < 1$ T, for the $\mathbf{H}||c$ direction. This is consistent with the vortex-lattice melting transitions generally observed in untwined YBa₂Cu₃O₇ crystals.²⁷ However, further thermodynamic evidence is necessary to support this claim.

In summary, our transport results show that H_{c2} is enhanced and the magnetic-field-induced broadening is significantly reduced in the large-grain polycrystalline bulk MgB₂ sample. Single-crystalline MgB₂ exhibits remarkable anisotropy in $H_{c2}(T)$ and $H^*(T)$ with $\gamma = H_{c2}^{ab}/H_{c2}^c \sim 3 \pm 0.2$. The large broadening of the superconducting transition for $\mathbf{H}||c$ direction indicates a significant suppression of $H^*(T)$ below H_{c2}^c for the same orientation. The sharp resistive transition and the sudden change of slope in *I-V* curves indicate the possibility of a first-order vortex-lattice melting like transition. These results could be very important to understand the mechanism of superconductivity in MgB₂ and useful for technological advances.

This work was supported by a Grant-in-aid for Scientific Research from the Ministry of Education, Culture, Sports, Science and Technology.

*Permanent address: Jesse W. Beams Laboratory of Physics, University of Virginia, Charlottesville, VA 22901.

†Corresponding author. Email address: tamegai@ap.t.u-tokyo.ac.jp

¹J. Nagamatsu *et al.*, Nature (London) **410**, 63 (2001).

²D.K. Finnemore *et al.*, Phys. Rev. Lett. **86**, 2420 (2001).

³S.L. Bud'ko *et al.*, Phys. Rev. Lett. **86**, 1877 (2001).

⁴D.C. Larbalestier *et al.*, Nature (London) **410**, 186 (2001).

⁵Y. Takano *et al.*, Appl. Phys. Lett. **78**, 2914 (2001).

⁶P.C. Canfield *et al.*, Phys. Rev. Lett. **86**, 2423 (2001).

⁷H.H. Wen *et al.*, Physica C **363**, 170 (2001).

⁸G. Fuchs *et al.*, Solid State Commun. **118**, 497 (2001).

⁹H. Haas and K. Maki, cond-mat/0104207 (unpublished).

¹⁰A. Handstein *et al.*, J. Alloys Compd. **329**, 285 (2001).

¹¹O.F. de Lima *et al.*, Phys. Rev. Lett. **86**, 5974 (2001).

¹²S. Patnaik *et al.*, Supercond. Sci. Technol. **14**, 315 (2001).

¹³M. Xu *et al.*, Appl. Phys. Lett. **79**, 2779 (2001).

¹⁴C.U. Jung, Jae-Hyuk Choi, P. Chowdhury, Kijoon H.P. Kim, Min-Seok Park, Heon-Jung Kim, J.Y. Kim, Zhonglian Du, Mun-Seog Kim, W.N. Kang, Sung-Ik Lee, Gun Yong Sung, and Jeong Yong

Lee, cond-mat/0105330 (unpublished).

¹⁵S. Lee *et al.*, J. Phys. Soc. Jpn. **70**, 2255 (2001).

¹⁶W.N. Kang *et al.*, Appl. Phys. Lett. **79**, 982 (2001).

¹⁷W.N. Kang, Hyeong-Jin Kim, Eun-Mi Choi, Kijoon H.P. Kim, and Sung-Ik Lee, cond-mat/0105024 (unpublished).

¹⁸R. Jin, M. Paranthaman, H.Y. Zhai, H.M. Christen, D.K. Christen, and D. Mandrus, cond-mat/0104411 (unpublished).

¹⁹Y. Takano, H. Takeya, H. Fujii, H. Kumakura, T. Hatano, K. Togano, H. Kito, and H. Ihara (unpublished).

²⁰F. Bouquet *et al.*, Phys. Rev. Lett. **87**, 047001 (2001).

²¹J. Kortus *et al.*, Phys. Rev. Lett. **86**, 4656 (2001).

²²F. Simon *et al.*, Phys. Rev. Lett. **87**, 047002 (2001).

²³Y. Bugoslavsky *et al.*, Nature (London) **411**, 561 (2001).

²⁴S.V. Shulga *et al.*, Phys. Rev. Lett. **80**, 1730 (1998).

²⁵H.-J. Kim *et al.*, Phys. Rev. Lett. **87**, 087002 (2001).

²⁶M.P.A. Fisher, Phys. Rev. Lett. **62**, 1415 (1989).

²⁷H. Safar *et al.*, Phys. Rev. Lett. **69**, 824 (1992); W.K. Kwok *et al.*, *ibid.*, **72**, 1088 (1994).